Universal Strategy to Develop Fluorogenic Probes for Lysine Deacylase/Demethylase Activity and Application in Discriminating Demethylation States

Wenyu Wei,[⊥] Jie Zhang,[⊥] Zhiqiang Xu, Zhiyang Liu, Chen Huang, Ke Cheng, Lingkuan Meng, Yudai Matsuda, Quan Hao, Huatang Zhang,* and Hongyan Sun*
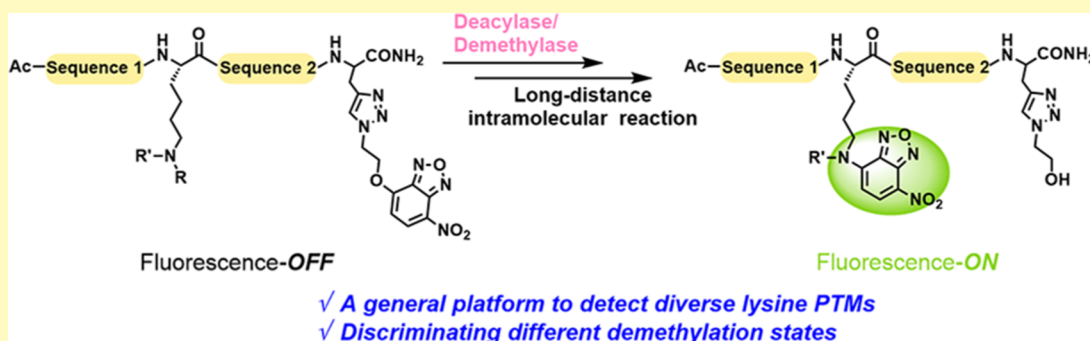
ACCESS | 📊 Metrics & More | 📖 Article Recommendations | 🆂�🅸 Supporting Information

√ A general platform to detect diverse lysine PTMs
√ Discriminating different demethylation states

ABSTRACT: Dynamically controlling the post-translational modification of the ε-amino groups of lysine residues is critical for regulating many cellular events. Increasing studies have revealed that many important diseases, including cancer and neurological disorders, are associated with the malfunction of lysine deacylases and demethylases. Developing fluorescent probes that are capable of detecting lysine deacylase and demethylase activity is highly useful for interrogating their roles in epigenetic regulation and diseases. Due to the distinct substrate recognition of these epigenetic eraser enzymes, designing a universal strategy for detecting their activity poses substantial difficulty. Moreover, designing activity-based probes for differentiating their demethylation states is even more challenging and still remains largely unexplored. Herein, we report a universal strategy to construct probes that can detect the enzymatic activity of epigenetic "erasers" through NBD-based long-distance intramolecular reactions. The probes can be easily prepared by installing the O-NBD group at the C-terminal residue of specific peptide substrates by click chemistry. Based on this strategy, detecting the activity of lysine deacetylase, desuccinylase, or demethylase with superior sensitivity and selectivity has been successfully achieved through single-step probe development. Furthermore, the demethylase probe based on this strategy is capable of distinguishing different demethylation states by both absorption and fluorescence lifetime readout. We envision that these newly developed probes will provide powerful tools to facilitate drug discovery in epigenetics in the future.

KEYWORDS: fluorogenic probe, post-translational modification, deacylase, desuccinylase, demethylase
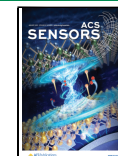
Post-translational modifications (PTMs) of the ε-amino group of lysine residues in proteins play diverse roles in the regulation of multiple biological processes in living cells. To date, a variety of lysine PTMs have been discovered, and many of them have been identified to play crucial roles in regulating cellular processes.[1,2] For example, lysine acetylation (Kac) is a key PTM involved in DNA replication and repair, and gene transcription.[3−6] Lysine succinylation (Ksucc) is known to modulate diverse metabolic pathways in mitochondria.[7,8] A variety of diseases, including cancer and cardiovascular diseases, are associated with Ksucc dysregulation.[9−11] Lysine crotonylation (Kcro) is found to be highly enriched in the regions of active promoters and enhancers.[12] Recently, lysine lactylation has been identified as a new histone PTM linked to inflammation and cancer.[13] Unlike lysine acetylation,

which is usually related to gene activation, lysine methylation can either activate or repress the genes depending on the sites and the states of methylation in histones.[14−16] Lysine methylation is closely involved in transcriptional regulation, heterochromatin assembly, and cell cycle progression.[17] In view of the fact that dynamic changes in histone acylation and methylation affect a variety of cellular functions, comprehen-
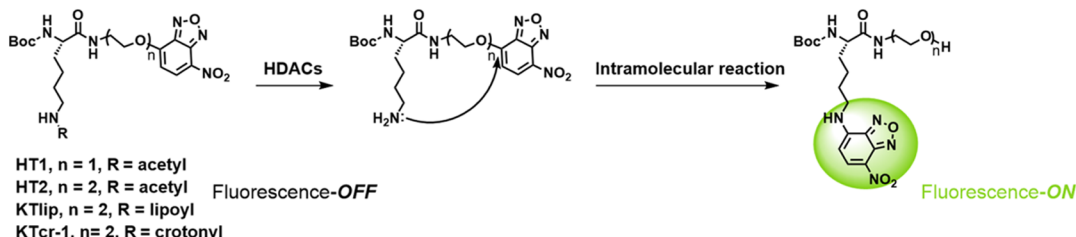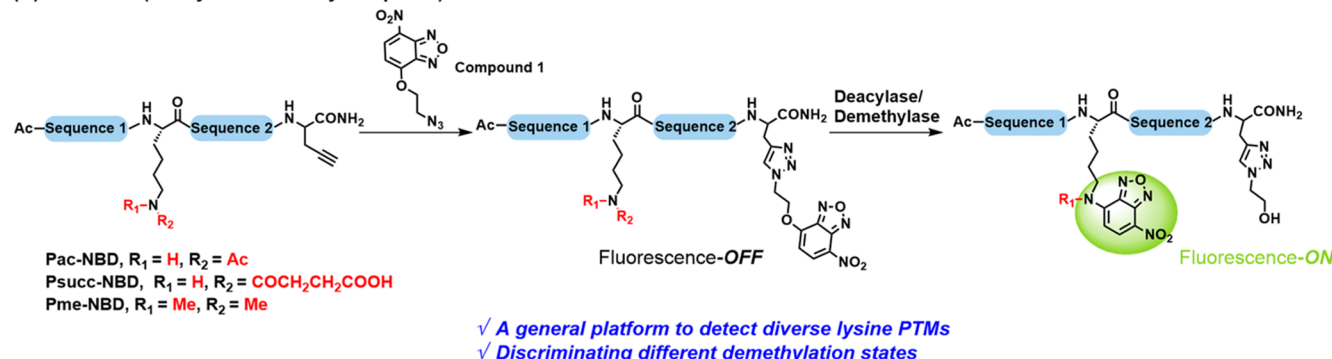
**Scheme 1. (A) Previous Work of NBD-Based Probes for Detecting Lysine Deacetylase, Delipoylase, and Decrotonylase (B) Universal Strategy for Designing Peptide-Based Fluorogenic Probes to Detect Deacetylase, Desuccinylase, and Demethylase**

(A) Our previous work

HT1, n = 1, R = acetyl
HT2, n = 2, R = acetyl
KTlip, n = 2, R = lipoyl
KTcr-1, n= 2, R = crotonyl

Fluorescence-OFF

Intramolecular reaction

Fluorescence-ON

(B) This work (Deacylase/ Demethylase probe)

Compound 1

Deacylase/ Demethylase

Pac-NBD, R₁ = H, R₂ = Ac
Psucc-NBD, R₁ = H, R₂ = COCH₂CH₂COOH
Pme-NBD, R₁ = Me, R₂ = Me

Fluorescence-OFF

Fluorescence-ON

√ A general platform to detect diverse lysine PTMs
√ Discriminating different demethylation states

sive characterization of their regulators (writers, erasers, and readers) is essential. It will help to fulfill the compelling need to deeply understand epigenetic regulation and its effects on disease progression.[18−21]

Histone deacetylases (HDACs) are epigenetic erasers that remove the acetyl groups from lysine residues in histones and nonhistone proteins.[22] Emerging evidence revealed that HDACs are capable of erasing various lysine acylations through enzymatic catalysis. For example, Sirt3 is found to erase lysine crotonylation.[23] Sirt5 has been identified as demalonylase/desuccinylase to erase malonylation/succinylation from lysine residues to regulate cellular metabolism.[24] Very recently, HDACs 1, 2, and 3 were identified as delactylases in HeLa cells.[25] Meanwhile, dysfunction of HDAC activity is frequently found in cancer and neurological diseases, making HDACs appealing drug targets for treating these pathologies.[26−28] Lysine methylation, on the other hand, is erased by the catalysis of lysine demethylases (KDMs).[18,29] For example, Jumonji C (JmjC) lysine demethylases are Fe(II)-dependent hydroxylases that catalyze the oxidative demethylation of methyl lysine residues in proteins.[30] Dysregulation of KDMs is associated with developmental disorders and various cancers.[31] As a result, KDMs have become the hot target for drug development.[32] Developing robust analytical methods to detect the enzymatic activity of lysine deacylases and demethylases will be beneficial to understand how these epigenetic erasers affect cellular activities.

To date, a number of methods for detecting HDAC and KDM activities have been developed, such as high-performance liquid chromatography (HPLC),[33] mass spectrometry (MS),[34] radioisotope methods,[35] and antibody-based methods.[36] However, these approaches have various drawbacks such as the need for expensive instruments, complicated experimental procedures, or multistep reactions. The fluorescence-

based method has emerged as a popular strategy to detect enzymatic activities due to its properties of facileness, high sensitivity, and high throughput. Therefore, researchers have shown strong interest in developing fluorescent probes to measure HDAC and KDM activities. For example, Schwienhorst et al. developed a coumarin-based substrate for fluorescence monitoring of HDAC activity.[37] This method, however, requires two steps involving trypsin digestion to produce fluorescence readout. Buccella and co-workers used intramolecular imine formation between a coumarin aldehyde and lysine residue to modulate fluorescence emission change to detect deacetylase and decrotonylase activity.[38,39] It was noted that the fluorescence turn-on fold was not high, potentially affecting the probe's sensitivity. Very recently, Kikuchi and co-workers successfully developed a series of novel fluorescent probes to measure lysine desuccinylase/demalonylase/demethylase activity based on the intramolecular reaction of 7-hydroxycoumarin and lysine residue.[40,41] However, this method requires installing 7-hydroxycoumarin at the N-terminus and the C-terminus of the peptide fragment, consequently increasing the complexity of probe design and the difficulty of synthesis. Due to the importance of HDACs and KDMs in diseases and the limited number of fluorescent probes to detect them, there has been an urgent need to develop new generations of fluorescent probes to measure their activity and delineate their complex roles in biology.

Our group has previously developed a series of fluorescent probes to detect various lysine deacylase activities. To construct these probes, a fluorescence switching group O-NBD group (NBD: nitrobenzoxadiazole) was incorporated into different lysine PTMs such as Kac, Klip, or Kcr residues with the PEG chain.[42−44] Using the O-NBD group offers some advantages: (1) the O-NBD moiety displays low fluorescence intensity, whereas the N-NBD group shows hyperfluorescence. Upon deacylation by HDACs, the released amine group

undergoes an intramolecular reaction with the O-NBD moiety, producing N-NBD with bright fluorescence. (2) The small size of the fluorophore minimizes the influence of target enzyme recognition and binding. (3) The NBD unit is not released and stays on the peptide. By integrating the photo-cross-linking strategy, we were able to develop dual-function probes for fluorescence labeling and enzyme detection simultaneously.[43] However, the previous design of NBD-based probes is limited to using short PEG linkers between lysine PTMs and fluorophore (Scheme 1A). This limitation hinders the development of probes for detecting enzymes with distinct substrate specificity because the activities of most epigenetic eraser enzymes rely on the recognition of long and diverse peptide sequences flanking the modified lysine site. For example, the previous version of our probes could not efficiently recognize Sirt3 and HDAC3/NCOR2, which are known erasers of Kac. A plausible reason is the lack of an appropriate peptide recognition sequence, which hinders the enzyme recognition process.

To tackle this problem, we herein introduce a long and diverse peptide sequence into our previous NBD-based platform by leveraging click chemistry. Our work revealed that with the long and diverse amino acid spacers between the lysine and the O-NBD group, the intramolecular reaction could still occur efficiently. Based on this principle, we designed a panel of NBD-based peptide probes for detecting deacetylase, desuccinylase, and demethylase activities by introducing the O-NBD group at the C-terminal of the peptides through click chemistry.[45] Altering the length and sequences of different peptide substrates allows detection of diverse enzymes including deacetylase, desuccinylase, and demethylase (Scheme 1B). This is a universal strategy and a facile method to construct peptide-based fluorogenic probes for detecting various epigenetic erasers. Apart from its potential to develop dual-function probes, our strategy also allows discrimination of different demethylation states for the first time based on absorption and lifetime readout.

EXPERIMENTAL SECTION

Materials and Instruments. All commercial materials were purchased from GL Biochem, Sigma-Aldrich, TCI, and J&K. The organic reaction was monitored using UV-based thin-layer chromatography (TLC). Bruker NMR spectrometers (300 and 400 MHz) were used to obtain ^{1}H and ^{13}C NMR spectra, respectively. An ESI mass spectrometer (SCIEX API) was utilized to acquire mass spectra. HPLC data were recorded on a Waters HPLC system equipped with an ultraviolet–visible (UV–vis) detector and a C18 reverse column. UV–vis absorption and fluorescence analysis were conducted using a Molecular Devices SpectraMax ID5 Microplate Reader. Fluorescence lifetime measurements were acquired on an Edinburgh FLS980 Spectrofluorometer. HDAC3/NCOR2 was purchased from Abcam. Recombinant Sirt1/2/3/5/6/7/JMJD2E was expressed and purified according to the previously reported methods.[24,41] KDM4DL (JMJD2E) plasmid was a gift from Nicola Burgess-Brown (RRID: Addgene_38990).

Enzymatic Reaction. **Pac-NBD** or **Psucc-NBD** was incubated with sirtuins and the cofactor NAD$^+$ in HEPES buffer (pH = 8.0, 20 mM HEPES) for the indicated period at 37 °C. **Pme-NBD** was incubated with JMJD2E enzyme for the specified time at 37 °C in HEPES buffer (pH = 8.0, 20 mM HEPES, 100 μM ammonium iron(II) sulfate, 500 μM 2-oxoglutaric acid, 2 mM ascorbate acid). After the enzyme and probes were incubated at 37 °C, the reactions were quenched with acetonitrile (containing 0.2% TFA) for RP-HPLC and ESI-MS analyses.

Measurement of Absorption and Fluorescence Spectra of Probes. The reaction was set to a total reaction volume of 200 μL. The absorbance spectra were collected in the range of 300 to 600 nm. The fluorescence spectra of enzymatic reactions using **Pac-NBD** or **Psucc-NBD** were collected from 520 to 700 nm using an excitation at 480 nm. On the other hand, the enzymatic reaction of **Pme-NBD** was measured between 535 and 850 nm using an excitation wavelength of 495 nm.

Determination of the First-Order Rate Constant _k_. The fluorescence data shown in Figures 3C,D, 4G, and S5D, S6D, S7D, S8D, and S11D were fitted to a first-order reaction equation to determine the first-order rate constant, k.

$$\text{normalized fluorescence intensity} = 1 - e^{-kt} \qquad (1)$$

Kinetic Study with Psucc-NBD Probe. **Psucc-NBD** (2.5, 5, 7.5, 10, 15, 20, 25, and 30 μM) was incubated with Sirt5 (0.1 μM) and NAD$^+$ (500 μM) in HEPES buffer at 37 °C. After the probe was mixed with the enzyme, the fluorescence intensities of the probe were monitored every 10 s (λ_{ex} = 480 nm; λ_{em} = 545 nm). The k_{cat} and K_m values for enzymatic reactions were determined by a modified Michaelis–Menten equation.[41] k_z is the rate constant of the intramolecular reaction of the model probe **PRM-5** (Figure S8D). B values at different probe concentrations were derived using eq 2 (Table S1). Subsequently, these data were fitted to derive k_{cat} and K_m values using eq 3 (Figure S4A).

$$F_t = F_0 + (F_{max} - F_0)(Ae^{-k_z t} + Bt - A)/[X]_0 \qquad (2)$$

$$B = \frac{k_{cat}[E]_0[X]}{K_m + [X]} \qquad (3)$$

where, F_t: observed fluorescence intensity; F_0: initial fluorescence intensity; F_{max}: maximum fluorescence intensity; A: constant; $[X]_0$: total concentration of the probe; k_z is 0.0015 s^{-1}, which is the rate constant of intramolecular reaction of the model peptide; $[E]_0$: concentration of enzyme; $[X]$: concentration of the probe; k_{cat}: turnover number; and K_m: Michaelis constant.

Kinetic Study with Psucc Peptide. Purified Sirt5 (0.1 μM) with NAD$^+$ (500 μM) was incubated at 37 °C for 20 min with increasing concentrations of **Psucc** peptide (0–250 μM) in HEPES buffer to determine the values of kinetic parameters. The reactions were quenched by adding 250 μL of acetonitrile containing 0.2% TFA and analyzed by HPLC with a gradient of 5–50% B (CH$_3$CN) over 25 min. The peak area at 200 nm was utilized to quantify the generated desuccinylated product. The values of k_{cat} and K_m were obtained through curve-fitting with the Michaelis–Menten equation.

Inhibition Assay. Increasing concentrations (0, 1, 10, 20, 40, 60, 80, 100, 150, and 300 μM) of the corresponding inhibitor (Tenovin-6 or suramin sodium) were first added to enzymes (Sirt2 or Sirt5) in HEPES buffer containing NAD$^+$ and incubated at 37 °C for 30 min. **Pac-NBD** or **Psucc-NBD** were then added and incubated for 1 h. Subsequently, the fluorescence of the reaction samples was measured. The percentage of the total activity of enzymes (Sirt2 or Sirt5) was calculated from the fluorescence intensity of samples at 545 nm relative to the positive control (without Tenovin-6 or suramin sodium). The IC$_{50}$ values were calculated on GraphPad Prism 9 software.

Fluorescence Lifetime Measurement. Fluorescence lifetime spectra were acquired on an FLS980 fluorescence spectrometer using an EPL-485 nm laser as the excitation source. Enzymatic reaction solutions of **Pme-NBD** probe (5 μM) reacted with low (0.8 μM) and high (10 μM) concentrations of JMJD2E were recorded after incubation at 37 °C for 2 h in HEPES buffer (pH = 8.0, 20 mM HEPES, 100 μM ammonium iron(II) sulfate, 500 μM 2-oxoglutaric acid, 2 mM ascorbate acid) at an excitation wavelength of 485 nm. Fluorescence lifetime values of NBD-N(Me)$_2$ (5 μM) and NBD-NHMe (5 μM) in HEPES buffer were recorded at an excitation wavelength of 485 nm. Fluorescence lifetime curves of NBD-N(Me)$_2$ (5 μM) and NBD-NHMe (5 μM) were obtained after being treated
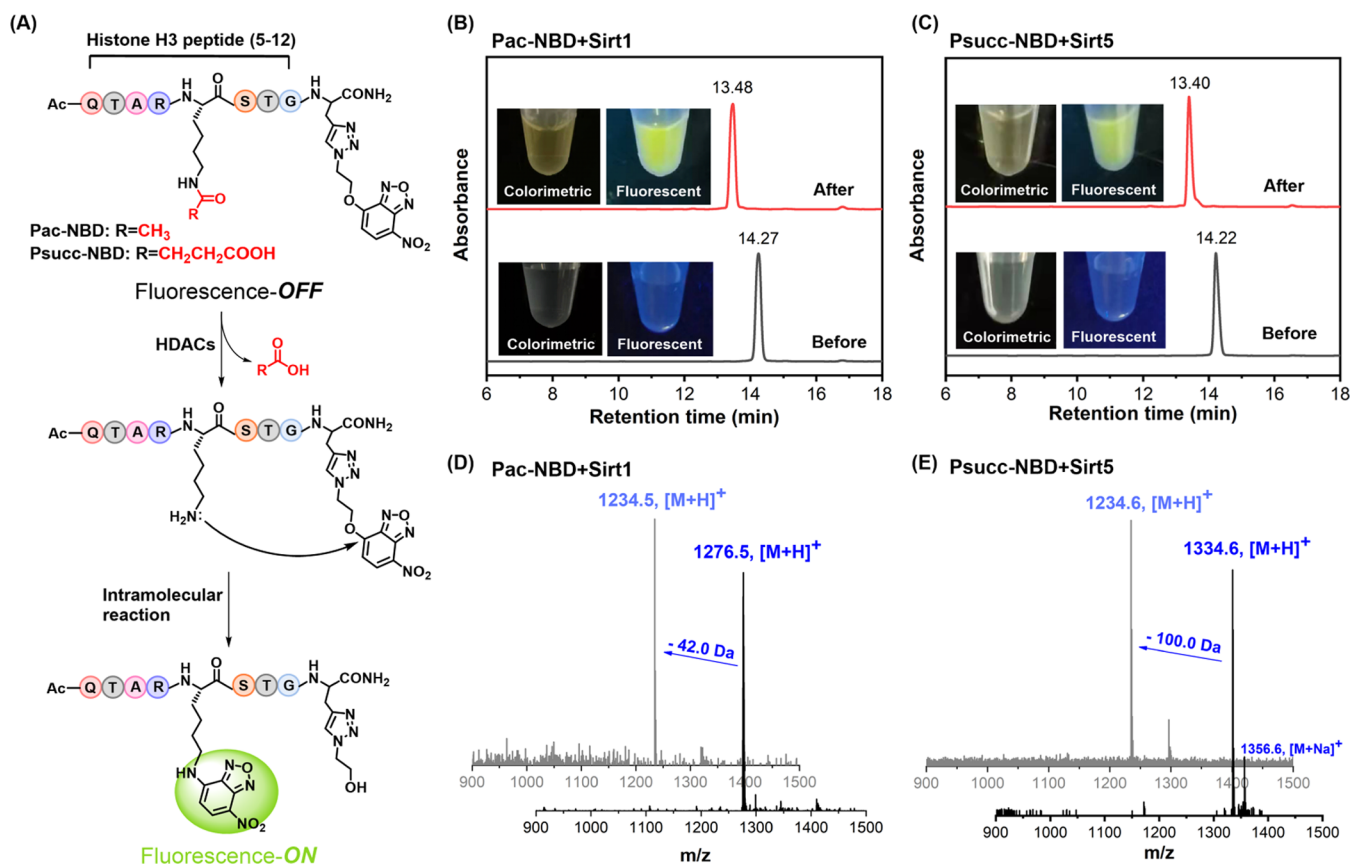
Figure 1. (A) Reaction mechanism of **Pac-NBD** and **Psucc-NBD** to detect enzymatic deacetylation and desuccinylation process. (B) HPLC analysis of the **Pac-NBD** probe with recombinant Sirt1 enzymatic reaction for 2 h in HEPES buffer containing 0.5 mM NAD^+. The inset in panel (B) shows the photographs of colorimetric and fluorescence changes of **Pac-NBD** solution before and after reaction with Sirt1. (C) HPLC analysis of the **Psucc-NBD** probe with recombinant Sirt5 enzymatic reaction for 2 h in HEPES buffer containing 0.5 mM NAD^+. The inset in panel (C) shows the photographs of colorimetric and fluorescence changes of **Psucc-NBD** solution before and after enzymatic reaction with Sirt5. (D) Mass analysis of **Pac-NBD** before and after enzymatic reaction. Left peak: 13.48 min peak after enzymatic reaction. Right peak: 14.27 min peak before enzymatic reaction. (E) Mass analysis of **Psucc-NBD** before and after enzymatic reaction. Left peak: 13.40 min peak after enzymatic reaction. Right peak: 14.22 min peak before enzymatic reaction.

with BSA (10 μM) for 2 h at 37 °C. The decay curves were fitted to an exponential equation.

RESULTS AND DISCUSSION

Design and Synthesis of Pac-NBD and Psucc-NBD. We first set out to design new generations of fluorogenic probes to detect lysine deacetylase and desuccinylase activities. To design a lysine deacetylase probe, the H3K9Ac sequence was chosen in our study as acetylation of H3K9 is known to be positively associated with gene expression.[46] As shown in Figure 1A, the O-NBD group was installed at the C-terminus of the H3K9Ac peptide through click chemistry to construct the deacetylase probe **Pac-NBD**. Using this probe as a model, we were able to examine whether the O-NBD group could efficiently react with the lysine residue after enzymatic deacetylation through a long-distance intramolecular reaction. On the other hand, lysine succinylation is another prevalent PTM that shows intriguing biological functions.[47] To detect the lysine desuccinylase activity, we designed **Psucc-NBD**, in which an H3K9Succ peptide was linked to the O-NBD group through click chemistry. Interestingly, H3K9 is also known to undergo succinylation and is a good substrate for Sirt5 (Figure 1A).[24] Such a probe will be useful to delineate the roles of lysine desuccinylase in cancers.

Reaction Mechanism Study of Pac-NBD and Psucc-NBD. After synthesizing **Pac-NBD** and **Psucc-NBD** by standard Fmoc solid-phase peptide synthesis (SPPS) and click chemistry (Schemes S2 and S3), the probes were purified by semipreparative HPLC and verified by LC-MS. We then moved on to the detailed study of the reaction mechanism of the probes with an enzyme. **Pac-NBD** and **Psucc-NBD** were incubated with their respective enzymes Sirt1 and Sirt5 in HEPES buffer in the presence of NAD^+, and the enzymatic reaction was monitored by HPLC. As shown in Figure 1B,C, the peaks of **Pac-NBD** and **Psucc-NBD** disappeared and new peaks appeared at 13.48 and 13.40 min, respectively, signifying the formation of new reaction products through enzymatic catalysis. Moreover, the colors of these two enzymatic reactions turned from colorless to yellow and showed strong green fluorescence, implying the formation of N-NBD fluorescent product (Figure 1B,C). Furthermore, the eluted fractions from HPLC analysis after the enzymatic reaction showed the mass peaks of the deacylated + substituted reaction products. The result agrees well with our previous experimental findings. Specifically, an expected 42.0 Da mass value shift was observed for **Pac-NBD**, and a 100.0 Da mass shift was observed for the **Psucc-NBD** probe (Figure 1D,E). These data together evidently demonstrated that peptide-based fluorogenic probes **Pac-NBD** and **Psucc-NBD** can be
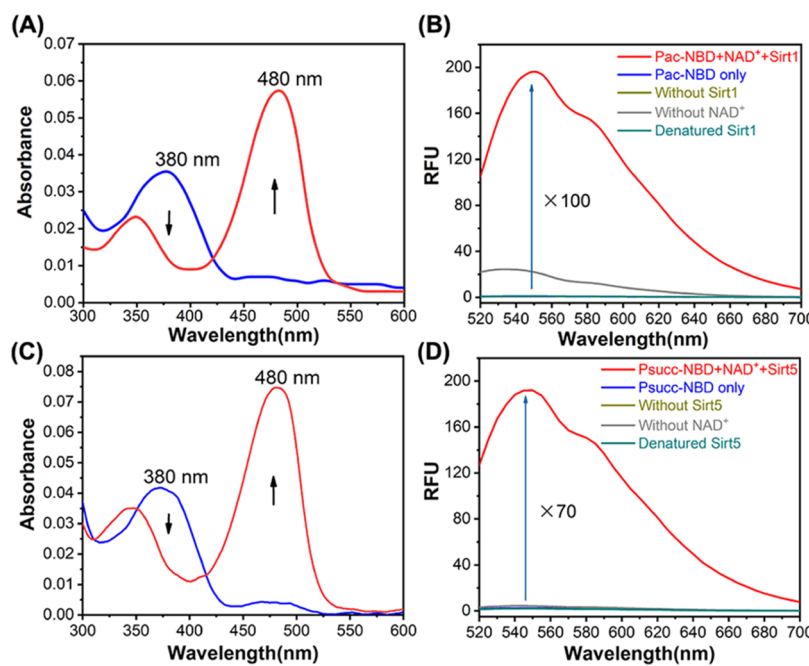
Figure 2. (A) Absorption spectra of the **Pac-NBD** probe (10 μM) before and after reaction with recombinant Sirt1 (0.1 μM) containing 100 μM NAD$^+$ for 2 h. (B) Fluorescence assay of the **Pac-NBD** probe (10 μM) with Sirt1 (0.1 μM) under various conditions (λ_{ex} = 480 nm). (C) Absorption spectra of the **Psucc-NBD** probe (10 μM) before and after enzymatic reaction with recombinant Sirt5 (0.1 μM) in 20 mM HEPES buffer (pH 8.0) containing 100 μM NAD$^+$ for 2 h. (D) Fluorescence assay of the **Psucc-NBD** probe (10 μM) with Sirt5 (0.1 μM) under various conditions (λ_{ex} = 480 nm).

efficiently recognized by the known Kac "eraser" Sirt1 and Ksucc "eraser" Sirt5, respectively. Gratifyingly, the long-distance intramolecular reactions between the O-NBD and $-NH_2$ groups in lysine residue occurred, despite the fact that there are three different amino acid residues between the Kacyl and O-NBD groups.

Enzymatic Assay with Pac-NBD and Psucc-NBD. We next performed detailed absorption and emission experiments of **Pac-NBD** and **Psucc-NBD** with their corresponding enzymes. First, an absorption peak could be found at 380 nm in **Pac-NBD** and **Psucc-NBD**. This absorption peak belongs to the O-NBD group. After the enzymatic reaction, a significant absorption peak at 480 nm appeared, indicating the successful formation of N-NBD (Figure 2A,C). Remarkably, strong turn-on fluorescence could be observed after the reaction of **Pac-NBD** with Sirt1(>100-fold) and **Psucc-NBD** with Sirt5 (>70-fold). In stark contrast, samples with probes only, probes with denatured enzymes, and probes without enzymes or NAD$^+$ displayed weak fluorescence or no fluorescence under 480 nm excitation wavelength (Figure 2B,D). HPLC analysis of the stability of **Pac-NBD** and **Psucc-NBD** showed that these probes were stable after prolonged incubation (>3 h) under physiological conditions (HEPES buffer, pH 8.0) (Figures S1A and S2A). In addition, the absorbance and fluorescence spectra also showed that the signals were almost the same after 3 h in HEPES buffer (pH 8.0) (Figures S1B,C and S2B,C), proving that the fluorescence signal originated from the enzyme-catalyzed reactions rather than environmental factors.

Selectivity Studies. We moved on to conduct selectivity studies of **Pac-NBD** and **Psucc-NBD** with various enzymes. Specifically, Sirt1, Sirt2, Sirt3, Sirt5, Sirt6, Sirt7, and HDAC3/NCOR2 were chosen for **Pac-NBD**, and Sirt1, Sirt2, Sirt3, Sirt5, Sirt6, and Sirt7 were selected for **Psucc-NBD**. Compared

with our previously developed probe HT1/HT2, in which the O-NBD group is linked to Kac through a PEG linker, the newly developed **Pac-NBD** is capable of not only sensing Sirt1 and Sirt2 but also detecting Sirt3 and HDAC3/NCOR2 activities with good response. On the other hand, no obvious activity was observed for Sirt5, Sirt6, and Sirt7 (Figure 3A). This phenomenon is consistent with the reported literature that H3K9Ac is a good substrate of deacetylases Sirt1, Sirt2, Sirt3, and HDAC3/NCOR2.[24] The result also underscores the importance of introducing an appropriate peptide sequence into the probe to improve the binding affinity of the enzyme and probe. In the case of **Psucc-NBD**, a better selectivity was observed. The fluorescence intensity of the probe increased only in the presence of Sirt5. No fluorescence increase was observed in the presence of other sirtuins, demonstrating that **Psucc-NBD** is highly selective toward Sirt5 (Figure 3B). Furthermore, we tested the selectivity of **Pac-NBD** and **Psucc-NBD** against other potential interferences, such as butylamine, cysteine, GSH, and BSA. The results showed that fluorescence enhancement was negligible with the above interferences, demonstrating the exquisite selectivity of our probes (Figure S3).

Kinetic and Inhibition Tests. Encouraged by the above results, we further examined the kinetics of the enzymatic reaction of **Pac-NBD** and **Psucc-NBD** by fluorescence analysis. The solution of probe **Pac-NBD** (Figure 3C) and **Psucc-NBD** (Figure 3D) displayed very weak fluorescence intensity initially. However, the fluorescence intensity increased rapidly and plateaued in 1 h. In contrast, no obvious fluorescence increase was observed in the absence of Sirt1/Sirt5. By fitting the fluorescence data to an exponential equation, the overall reaction rate (k_{oval}) of the fluorescent product generated through both enzyme catalysis and intramolecular nucleophilic reaction was determined to be
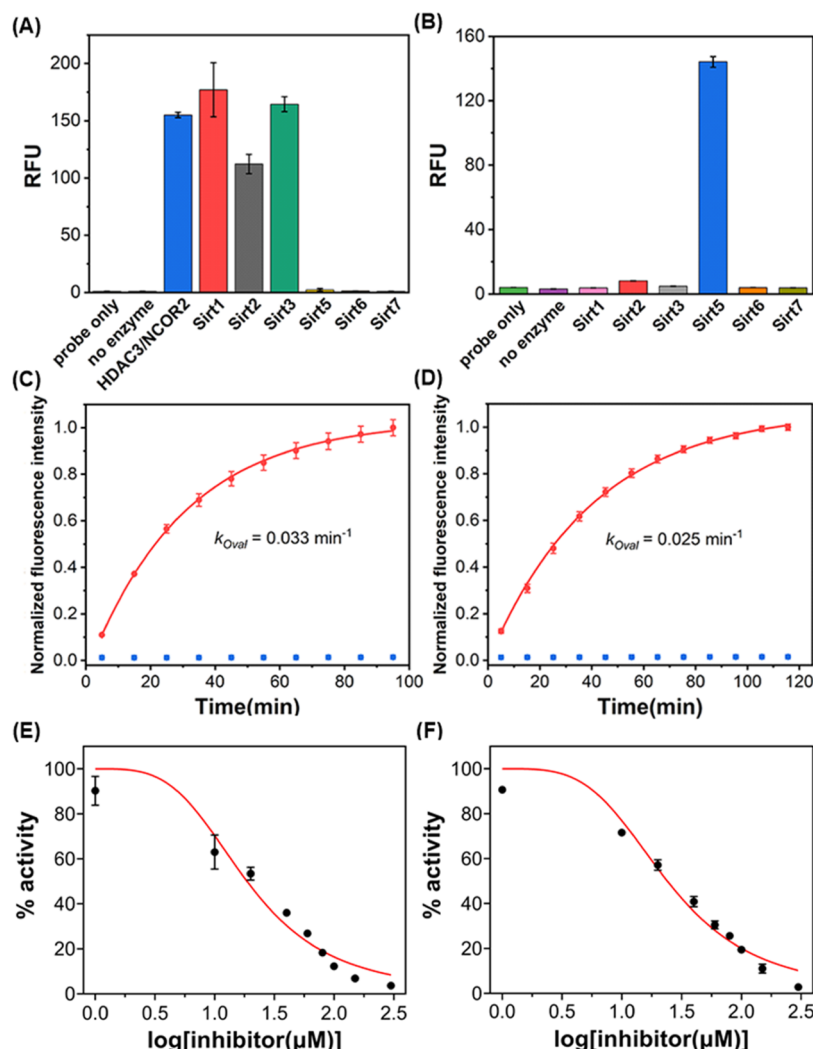
Figure 3. (A) Fluorescence detection of **Pac-NBD** (10 μM) with different HDACs (enzyme concentration: 0.1 μM, λ_{ex} = 480 nm; λ_{em} = 545 nm) at 37 °C for 1 h. (B) Fluorescence detection of **Psucc-NBD** (10 μM) with different sirtuins (enzyme concentration: 0.1 μM, λ_{ex} = 480 nm; λ_{em} = 545 nm) at 37 °C for 1 h. (C) Time-dependent fluorescence measurements of **Pac-NBD** (10 μM) in the presence (red) and absence (blue) of Sirt1 (λ_{ex} = 480 nm; λ_{em} = 545 nm). (D) Time-dependent fluorescence measurements of **Psucc-NBD** (10 μM) in the presence (red) and absence (blue) of Sirt5 (λ_{ex} = 480 nm; λ_{em} = 545 nm). (E) The dose−response inhibition curve of Sirt2 deacetylation activity by Tenovin-6 using **Pac-NBD** (10 μM). (F) The dose−response inhibition curve of Sirt5 desuccinylation activity by suramin sodium using **Psucc-NBD** (10 μM). Values of the Y axis correspond to the average enzyme activity of three independent experiments.

0.033 min^{-1} for Sirt1 and 0.025 min^{-1} for Sirt5. Moreover, enzyme kinetic parameters for the catalysis reaction of Sirt5 toward **Psucc-NBD** were determined using a modified Michaelis−Menten equation.[41] The turnover number (k_{cat}) and Michaelis constant (K_m) of **Psucc-NBD** toward Sirt5 were calculated to be 0.122 s^{-1} and 11.7 μM, respectively, using the fluorescence method (Tables S1 and S2, and Figure S4A). These kinetic parameters were very similar to that of a natural **Psucc** peptide substrate using the HPLC assay (Figure S4B). The results showed that introducing the O-NBD group at the C-terminal of the peptide causes little change in kinetic parameters (Table S2). It also indicated that NBD-based peptide probes can become a practical tool for detecting HDAC activity. Furthermore, **Pac-NBD** and **Psucc-NBD** were investigated for their ability to evaluate the inhibition potency of sirtuin inhibitors. Tenovin-6 and Suramin sodium, two well-known inhibitors of Sirt2 and Sirt5, were chosen. Different concentrations (0, 1, 10, 20, 40, 60, 80, 100, 150, and 300 μM) of inhibitors were incubated with the enzymes (Sirt2 or Sirt5)

for 30 min. **Pac-NBD** or **Psucc-NBD** were then added and incubated for one hour. The fluorescence intensity of the reaction solution was measured, and the data were fitted into the equation to derive the IC$_{50}$ values of Tenovin-6 and Suramin, which were determined to be 18.66 μM (Figures 3E) and 24.10 μM (Figure 3F), respectively. These IC$_{50}$ values are close to the reported values, indicating that **Pac-NBD** and **Psucc-NBD** can serve as invaluable tools to detect the enzymatic activity of HDACs and related drug discovery development.[43,44,48,49] Taken together, all results consistently demonstrated that single-step probes **Pac-NBD** and **Psucc-NBD** are robust chemical tools for detecting lysine deacetylase and desuccinylase activities.

Model Studies with PRM. To evaluate the effect of the linker length on the intramolecular substitution reaction between the lysine and O-NBD, three model probes **PRM-1**, **PRM-2**, and **PRM-3** were synthesized following Scheme S5. Subsequently, fluorescence signal changes were closely monitored when these probes were incubated with HEPES
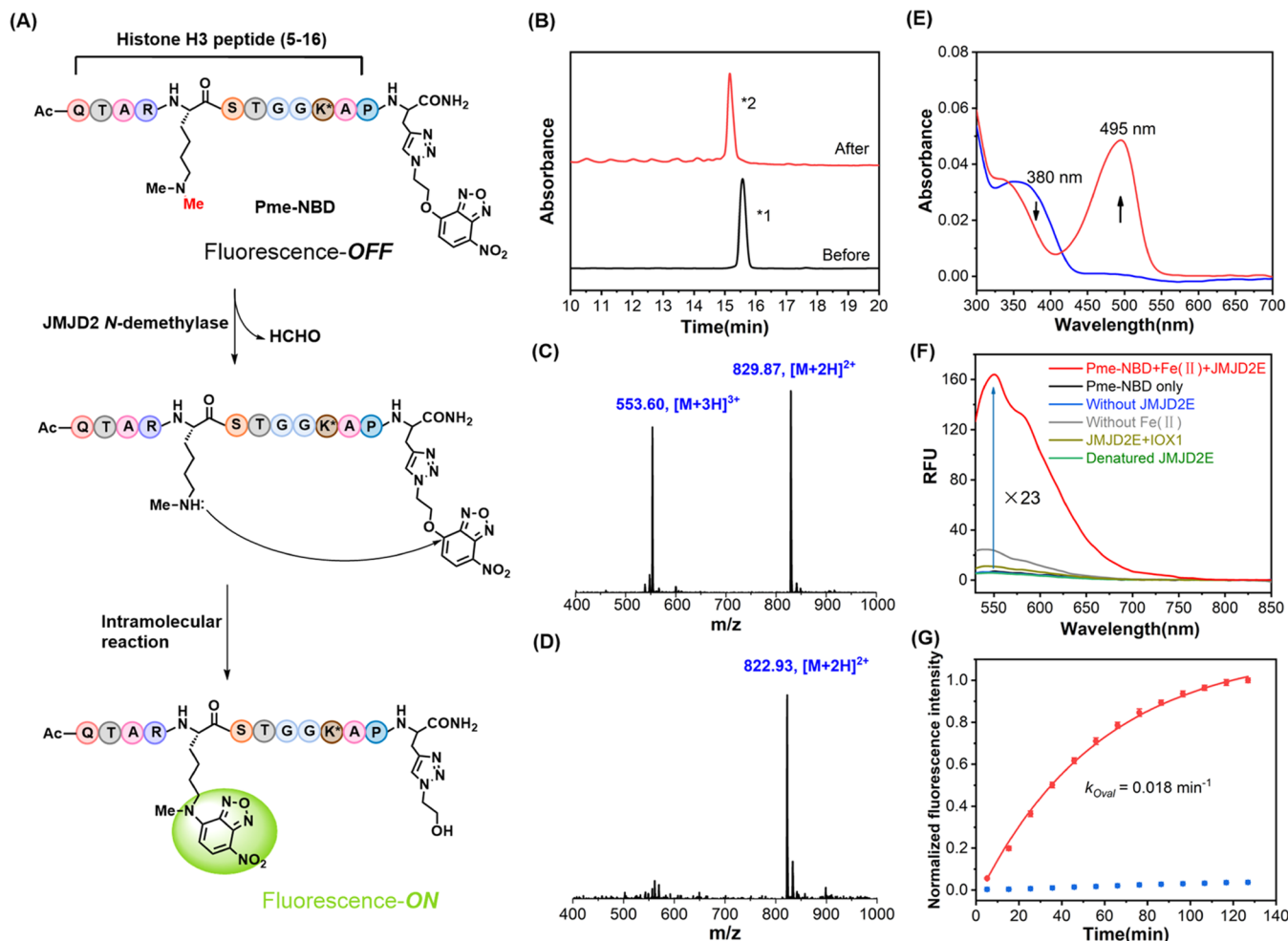
Figure 4. (A) Schematic representation of a long-distance intramolecular reaction to detect JMJD2E enzymatic reaction using a single-step fluorescent probe. The peptide sequence used is the histone H3K9Me$_2$ peptide (amino acids 5−16). The 14th position of the acetylated lysine is marked with an asterisk. (B) HPLC analysis of the enzymatic reaction of the **Pme-NBD** probe (15 μM) with recombinant JMJD2E (3 μM) in HEPES buffer containing 200 μM Fe^{2+}, 1 mM 2-OG, and 2 mM ascorbate acid at 37 °C for 3 h. The retention time of the peaks marked with asterisks 1 and 2 is 15.57 and 15.17 min, respectively. (C) Mass spectrum of peak 1 in LC analysis. (D) The mass spectrum of peak 2 in LC analysis. (E) Absorption spectra of the **Pme-NBD** probe (5 μM) before and after enzymatic reaction with JMJD2E (0.8 μM) for 3 h. (F) The fluorescence assay of the **Pme-NBD** probe (5 μM) with or without JMJD2E (0.8 μM) under various conditions (λ_{ex} = 495 nm). (G) Time-dependent fluorescence measurements of **Pme-NBD** (5 μM) in the presence (red) and absence (blue) of JMJD2E (λ_{ex} = 495 nm; λ_{em} = 550 nm).

buffer (pH = 8.0). By fitting the fluorescence data to an exponential equation, the first-order rate constant (k) of **PRM-1**, **PRM-2**, and **PRM-3** was determined to be 0.046, 0.034, and 0.033 min^{-1}, respectively (Figures S5D, S6D, and S7D). It was noticed that **PRM-1** with a one amino acid spacer showed slightly better intramolecular substitution reaction kinetic (0.046 min^{-1}) than those with longer spacers. Furthermore, **PRM-2** with a three amino acid spacer and **PRM-3** with a seven amino acid spacer showed very similar reaction kinetics. Spacer elongation did not cause a significant decrease in the reaction kinetics (Table S3, and Figures S5−S7). Subsequently, **PRM-5** containing the same distance between lysine and NBD but different sequences with **PRM-2** was also synthesized to explore the effect of the peptide sequence on the reaction rate of the probe (Scheme S6). Interestingly, **PRM-5**, which contains the H3K9(5−12) peptide sequence, showed slightly better kinetics than **PRM-2**, indicating that peptide sequence may affect the reaction rate of intramolecular substitution to some extent (Table S3, and Figures S6 and S8). In summary, the intramolecular substitution reaction of O-

NBD shows rapid kinetics and is suitable to design probes for long-distance (at least seven amino acid spacer) peptide substrates with various sequences. This intramolecular substitution reaction shows broad applicability in probe design.

Design and Synthesis of Pme-NBD. Lysine methylation, which is heavily involved in epigenetic chromatin modifications, is one of the most important lysine PTMs. Apart from establishing different chromatin states, the methylation of histone tails promotes gene silencing and activation. Developing a lysine demethylase probe is therefore crucial for deciphering the functions of demethylases as well as facilitating future drug discovery in epigenetics.[50] However, lysine demethylases exhibit much stricter peptide sequence specificity than lysine deacylases do, posing a significant challenge for the development of demethylase probes.[51−53]

Preliminary Study of the O-NBD Group with Monomethylated, Dimethylated, and Trimethylated Lysines. To verify whether the NBD-based platform can be used for detecting demethylase activity, we first examined the reactivity of the O-NBD group and tri-, di-, and mono-
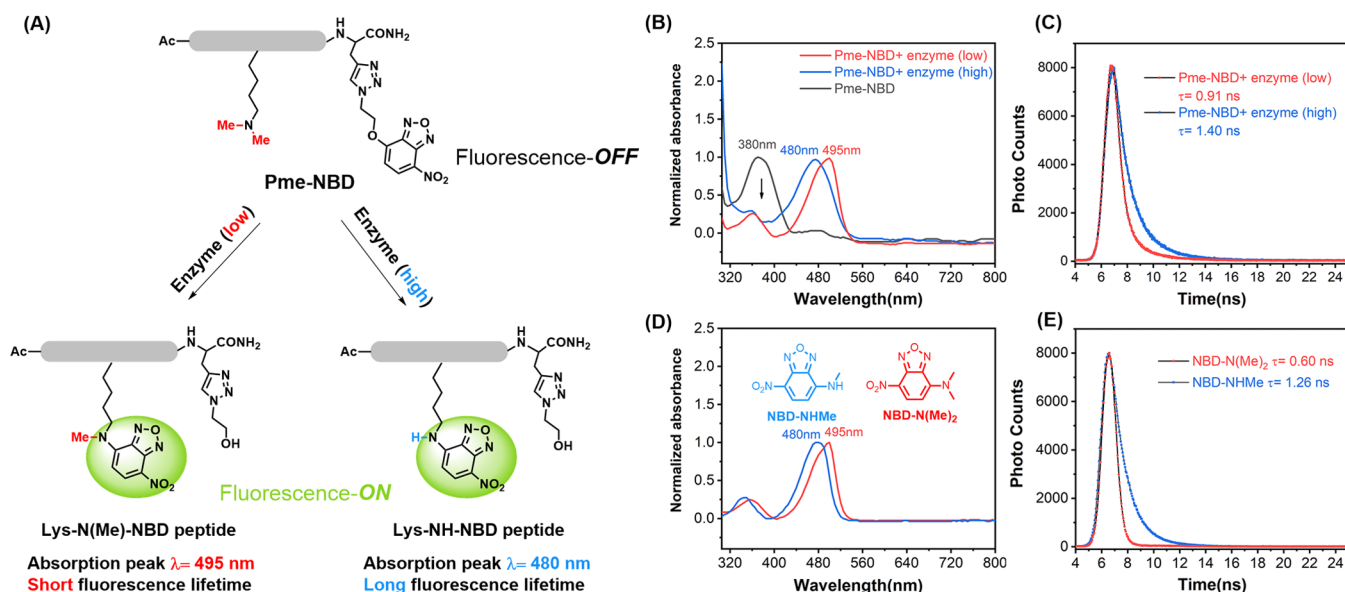
Figure 5. (A) Schematic illustration of discriminating demethylation states using the **Pme-NBD** probe. (B) Absorption spectra and (C) fluorescence lifetime of the **Pme-NBD** probe (5 μM) after enzymatic reaction with low (0.8 μM) and high (10 μM) concentrations of JMJD2E. Absorption spectra (D) and fluorescence lifetime (E) of synthetic small molecule NBD-amine analogues (NBD-N(Me)$_2$ and NBD-NHMe).

methylated amines through absorption and fluorescence studies. As shown in Figure S9A, the O-NBD group itself has an absorption peak at 380 nm. After adding high concentrations of monomethylated lysine, a new peak at around 495 nm was detected. Compared with Lys-NH-NBD, it showed a red shift of absorption wavelength. In addition, the fluorescence intensity of the reaction with monomethylated lysine increased over time when excited at 495 nm (Figure S9B). These phenomena suggest that monomethylated lysine could react with O-NBD to form the fluorescent reaction product. In contrast, trimethylated or dimethylated lysine and O-NBD reaction did not show obvious changes in absorbance and fluorescence after 24 h of incubation (Figure S10). These results reveal the different reactivities of monomethylated, dimethylated, and trimethylated lysine toward O-NBD and suggest high feasibility of our approach for demethylase probe development. The model probe **PRM-4**, which contains a seven amino acid distance spacer between monomethylated lysine and the O-NBD group, was next synthesized to investigate the kinetic of the intramolecular substitution reaction (Scheme S5). As shown in Figure S11, after adjusting pH to 8.0, HPLC produced a new peak, and the absorption peak shifted to 495 nm rapidly, which is the characteristic peak of monomethylated lysine and O-NBD reaction. At pH 8.0, significant fluorescence enhancement could be observed and the first-order rate constant (k) was determined to be 0.26 min^{-1} by fitting the fluorescence data to an exponential equation. In contrast, the fluorescence intensity did not show an obvious change under pH 2.0. All of the experiments indicated that the NBD-based peptide probes, in addition to detecting HDAC activity, have high potential applicability for detecting demethylases.

Due to the stringent substrate specificity of lysine demethylase, we opted to incorporate histone H3K9Me$_2$ (5–16) peptide sequence containing dimethylated lysine into our probe design.[54] Notably, a long amino acid spacer is inserted between dimethylated lysine and O-NBD fluorophore to achieve high binding affinity of the target enzyme and the

probe. We hypothesize that the dimethylated lysine will be converted to monomethylated lysine by demethylase. Subsequently, the monomethylated lysine will undergo long-distance intramolecular exchange spontaneously with the O-NBD group and turn on the fluorescence (Figure 4A).

Enzymatic Assay with Pme-NBD. Pme-NBD was synthesized by Fmoc chemistry combined with click chemistry, as previously described (Scheme S4). The probe was purified by semipreparative HPLC and then characterized by LC-MS. After obtaining the probe, we first performed HPLC analysis of enzymatic reaction of **Pme-NBD** and JMJD2E. The enzymatic reaction was incubated in 20 mM HEPES buffer (pH 8.0) at 37 °C for 3 h. As expected, the peak corresponding to **Pme-NBD** decreased after adding JMJD2E. Instead, a new peak with a retention time of 15.17 min appeared (Figure 4B). Further, MS analysis of this new peak displayed the expected 14.0 Da shift compared with the MS peak of **Pme-NBD** itself. These results together indicate that JMJD2E can recognize and catalyze the demethylation of **Pme-NBD**. Notably, the expected demethylated/exchanged product was generated (Figure 4C,D). Despite the fact that the spacer contains seven different amino acids, long-distance intramolecular reactions still occurred between the O-NBD group and the monomethylated lysine.

Next, we carried out detailed absorption and fluorescence study with **Pme-NBD** and JMJD2E. Briefly, **Pme-NBD** and JMJD2E were incubated in a solution (HEPES, pH 8.0) containing 100 μM Fe^{2+}, 500 μM 2-OG, and 2 mM ascorbate acid at 37 °C. The solution initially exhibited an absorption peak at 380 nm. After 3 hours of enzymatic reaction with JMJD2E, a new absorption peak was detected at 495 nm, which is the characteristic peak of Lys-N(Me)-NBD (Figure 4E). Subsequently, fluorescence measurements were carried out (Figure 4F). After JMJD2E and cofactor Fe^{2+} were added, significant fluorescence enhancement could be observed. The fluorescence turn-on fold was 23-fold at an emission wavelength of 550 nm. In stark contrast, probes only, probes with denatured enzymes, and probes without enzymes or Fe^{2+}

displayed weak fluorescence or no fluorescence (Figure 4F). Further, the time-dependent fluorescence test revealed that the fluorescence intensity of **Pme-NBD** and JMJD2E increased gradually with an increasing incubation time (Figure 4G). The overall reaction rate (k_{oval}) of the fluorescent product was calculated to be 0.018 min^{-1}. The inhibition study with a JMJD2E inhibitor IOX1 showed that the fluorescence intensity of the reaction of **Pme-NBD** and JMJD2E was greatly suppressed in the presence of the inhibitor (Figure 4F). Furthermore, HPLC, absorbance, and fluorescence studies all showed that **Pme-NBD** exhibited excellent stability (Figure S12). These data unambiguously proved that **Pme-NBD** can serve as a useful tool to detect demethylase activity and the above fluorescence turn-on is attributed to enzyme activity rather than environmental factors.

Discriminating Demethylation States with Pme-NBD. Developing activity-based probes for distinguishing the demethylation states of KDMs presents a significant challenge in the field of PTMs. Different methylation states could have different effects on gene expression and transcription.[55,56] We next proceeded to evaluate the potential of **Pme-NBD** to discriminate demethylation states (Figure 5A). Interestingly, we found that high concentrations of JMJD2E could result in the removal of two methyl groups from the dimethylated **Pme** peptide substrate, which is also confirmed by ESI-MS (Figure S13), while it removes a single methyl group at low concentrations.[57] This finding suggests that demethylation states can be controlled using different concentrations of JMJD2E. To distinguish demethylation states, we treated **Pme-NBD** with different concentrations of JMJD2E and then measured the absorption spectra. As shown in Figure 5B, when treated with low concentrations of enzyme, **Pme-NBD** showed an absorption peak at 495 nm, signifying single removal of the methyl group and the formation of Lys-N(Me)-NBD in the peptide. On the other hand, **Pme-NBD** treated with high concentrations of JMJD2E showed an absorption peak at 480 nm and the loss of the two-methyl group in the **Pme-NBD** probe was observed in mass analysis after demethylation, suggesting complete removal of methyl groups and formation of Lys-NH-NBD in the peptide (Figures 5B and S14). In addition, the fluorescence lifetime of the two reaction products was also measured accordingly (Figure 5C). Results showed that Lys-N(Me)-NBD peptide possessed a shorter fluorescence lifetime (τ = 0.91 ns) compared with Lys-NH-NBD peptide (τ = 1.40 ns). The difference in absorption and fluorescence lifetime was further confirmed by studying the photophysical properties of two small molecule NBD analogues, NBD-NHMe and NBD-N(Me)$_2$. The two small molecules exhibited similar absorption properties and fluorescence lifetime to their counterparts Lys-NH-NBD and Lys-N(Me)-NBD peptide products (Figure 5D,E). Furthermore, there was negligible fluorescence labeling of the enzyme after incubating **Pme-NBD** and JMJD2E, ruling out the interference of proximity labeling with the enzyme (Figure S15). Incubation of NBD analogues with BSA has no effect on the absorption and fluorescence lifetime, indicating no disturbance of the signals caused by nonspecific protein binding (Figures S16 and S17). These experimental data strongly demonstrated that **Pme-NBD** is capable of discriminating the demethylation states of demethylase in an activity-based manner.

CONCLUSIONS

In summary, we discovered that long-distance intramolecular reactions can occur efficiently with long amino acid spacers between the O-NBD group and unmodified lysine residue under mild aqueous conditions. On this basis, we have developed a new and universal NBD-based platform that can be conveniently used for reporting HDAC and KDM activities. Specifically, we have designed and constructed three activity-based fluorescent peptide probes (**Pac-NBD**, **Psucc-NBD**, and **Pme-NBD**) to detect enzymatic activities of deacetylase, desuccinylase, and demethylase with high sensitivity and selectivity. By a simple process of mix−react−read, the probes are capable of monitoring the activity of HDACs or JMJD2E in real time. These probes can be used to assess the inhibitors of the corresponding enzymes in a high-throughput manner. Notably, the demethylase probe successfully discriminated the demethylation states under different enzyme concentrations in an activity-based manner. Furthermore, our NBD-based platform can be readily extended to study the enzymatic activity of epigenetic erasers that remove other novel lysine PTMs such as lysine lactylation, lysine isonicotinylation, etc.[13,58] This will help to further elucidate their biological roles. We anticipate that our newly developed probes will provide powerful tools to efficiently analyze various lysine deacylases and demethylases activity and accelerate epigenetic drug development in the future.

ASSOCIATED CONTENT

ⓈI Supporting Information

The Supporting Information is available free of charge at https://pubs.acs.org/doi/10.1021/acssensors.2c01345.

> Synthesis and purification of probes; stability of probes; synthesis of model probes; kinetic analysis of Sirt5 toward the **Psucc-NBD** probe and **Psucc** peptide; kinetics of model probes; MS analysis of the **Pme-NBD** probe and **Pme** peptide with a high concentration of the enzyme; and NMR and MS spectra of **Compound 1** (PDF)

AUTHOR INFORMATION

Corresponding Authors

Huatang Zhang − School of Chemical Engineering and Light Industry, Guangdong University of Technology, Guangzhou, Guangdong 510006, China; ⓞ orcid.org/0000-0002-9556-2094; Email: htzhang@gdut.edu.cn

Hongyan Sun − Department of Chemistry and COSADAF (Centre of Super-Diamond and Advanced Films), City University of Hong Kong, Kowloon, Hong Kong 999077, China; Key Laboratory of Biochip Technology, Biotech and Health Centre, Shenzhen Research Institute of City University of Hong Kong, Shenzhen 518057, China; ⓞ orcid.org/0000-0003-0932-6405; Email: hongysun@cityu.edu.hk

Authors

Wenyu Wei − Department of Chemistry and COSADAF (Centre of Super-Diamond and Advanced Films), City University of Hong Kong, Kowloon, Hong Kong 999077, China; Key Laboratory of Biochip Technology, Biotech and Health Centre, Shenzhen Research Institute of City University of Hong Kong, Shenzhen 518057, China

Jie Zhang − Department of Chemistry and COSADAF (Centre of Super-Diamond and Advanced Films), City

University of Hong Kong, Kowloon, Hong Kong 999077, China; Key Laboratory of Biochip Technology, Biotech and Health Centre, Shenzhen Research Institute of City University of Hong Kong, Shenzhen 518057, China

Zhiqiang Xu − *Department of Chemistry and COSADAF (Centre of Super-Diamond and Advanced Films), City University of Hong Kong, Kowloon, Hong Kong 999077, China; Key Laboratory of Biochip Technology, Biotech and Health Centre, Shenzhen Research Institute of City University of Hong Kong, Shenzhen 518057, China*

Zhiyang Liu − *Department of Chemistry and COSADAF (Centre of Super-Diamond and Advanced Films), City University of Hong Kong, Kowloon, Hong Kong 999077, China; Key Laboratory of Biochip Technology, Biotech and Health Centre, Shenzhen Research Institute of City University of Hong Kong, Shenzhen 518057, China*

Chen Huang − *Department of Chemistry and COSADAF (Centre of Super-Diamond and Advanced Films), City University of Hong Kong, Kowloon, Hong Kong 999077, China; Key Laboratory of Biochip Technology, Biotech and Health Centre, Shenzhen Research Institute of City University of Hong Kong, Shenzhen 518057, China*

Ke Cheng − *Department of Chemistry and COSADAF (Centre of Super-Diamond and Advanced Films), City University of Hong Kong, Kowloon, Hong Kong 999077, China; Key Laboratory of Biochip Technology, Biotech and Health Centre, Shenzhen Research Institute of City University of Hong Kong, Shenzhen 518057, China*

Lingkuan Meng − *Department of Chemistry and COSADAF (Centre of Super-Diamond and Advanced Films), City University of Hong Kong, Kowloon, Hong Kong 999077, China; Key Laboratory of Biochip Technology, Biotech and Health Centre, Shenzhen Research Institute of City University of Hong Kong, Shenzhen 518057, China*

Yudai Matsuda − *Department of Chemistry and COSADAF (Centre of Super-Diamond and Advanced Films), City University of Hong Kong, Kowloon, Hong Kong 999077, China;* ⓘ orcid.org/0000-0001-5650-4732

Quan Hao − *Department of Physiology, University of Hong Kong, Pok Fu Lam, Hong Kong 999077, China*

Complete contact information is available at:
https://pubs.acs.org/10.1021/acssensors.2c01345

Author Contributions

[⊥]W.W. and J.Z. contributed equally to this work.

Notes

The authors declare no competing financial interest.

■ ACKNOWLEDGMENTS

■ REFERENCES

(1) Musselman, C. A.; Lalonde, M. E.; Cote, J.; Kutateladze, T. G. Perceiving the epigenetic landscape through histone readers. *Nat. Struct. Mol. Biol.* **2012**, *19*, 1218−1227.

(2) Diehl, K. L.; Muir, T. W. Chromatin as a key consumer in the metabolite economy. *Nat. Chem. Biol.* **2020**, *16*, 620−629.

(3) Lin, C. C.; Kitagawa, M.; Tang, X.; Hou, M. H.; Wu, J.; Qu, D. C.; Srinivas, V.; Liu, X.; Thompson, J. W.; Mathey-Prevot, B.; et al. CoA synthase regulates mitotic fidelity via CBP-mediated acetylation. *Nat. Commun.* **2018**, *9*, No. 1039.

(4) Wang, Z.; Yang, X.; Liu, C.; Li, X.; Zhang, B.; Wang, B.; Zhang, Y.; Song, C.; Zhang, T.; Liu, M.; et al. Acetylation of PHF5A Modulates Stress Responses and Colorectal Carcinogenesis through Alternative Splicing-Mediated Upregulation of KDM3A. *Mol. Cell* **2019**, *74*, 1250−1263.

(5) Shvedunova, M.; Akhtar, A. Modulation of cellular processes by histone and non-histone protein acetylation. *Nat. Rev. Mol. Cell Biol.* **2022**, *23*, 329−349.

(6) Chen, H.; Zhao, Y. F.; Chen, Y. X.; Li, Y. M. Exploring the Roles of Post-Translational Modifications in the Pathogenesis of Parkinson's Disease Using Synthetic and Semisynthetic Modified alpha-Synuclein. *ACS Chem. Neurosci.* **2019**, *10*, 910−921.

(7) Zhang, Z.; Tan, M.; Xie, Z.; Dai, L.; Chen, Y.; Zhao, Y. Identification of lysine succinylation as a new post-translational modification. *Nat. Chem. Biol.* **2011**, *7*, 58−63.

(8) Yang, Y.; Tapias, V.; Acosta, D.; Xu, H.; Chen, H.; Bhawal, R.; Anderson, E. T.; Ivanova, E.; Lin, H.; Sagdullaev, B. T.; et al. Altered succinylation of mitochondrial proteins, APP and tau in Alzheimer's disease. *Nat. Commun.* **2022**, *13*, No. 159.

(9) Yang, X.; Wang, Z.; Li, X.; Liu, B.; Liu, M.; Liu, L.; Chen, S.; Ren, M.; Wang, Y.; Yu, M.; et al. SHMT2 Desuccinylation by SIRT5 Drives Cancer Cell Proliferation. *Cancer Res.* **2018**, *78*, 372−386.

(10) Sadhukhan, S.; Liu, X.; Ryu, D.; Nelson, O. D.; Stupinski, J. A.; Li, Z.; Chen, W.; Zhang, S.; Weiss, R. S.; Locasale, J. W.; et al. Metabolomics-assisted proteomics identifies succinylation and SIRT5 as important regulators of cardiac function. *Proc. Natl. Acad. Sci. U.S.A.* **2016**, *113*, 4320−4325.

(11) Yang, L.; Peltier, R.; Zhang, M.; Song, D.; Huang, H.; Chen, G.; Chen, Y.; Zhou, F.; Hao, Q.; Bian, L.; et al. Desuccinylation-Triggered Peptide Self-Assembly: Live Cell Imaging of SIRT5 Activity and Mitochondrial Activity Modulation. *J. Am. Chem. Soc.* **2020**, *142*, 18150−18159.

(12) Tan, M.; Luo, H.; Lee, S.; Jin, F.; Yang, J. S.; Montellier, E.; Buchou, T.; Cheng, Z.; Rousseaux, S.; Rajagopal, N.; et al. Identification of 67 histone marks and histone lysine crotonylation as a new type of histone modification. *Cell* **2011**, *146*, 1016−1028.

(13) Zhang, D.; Tang, Z.; Huang, H.; Zhou, G.; Cui, C.; Weng, Y.; Liu, W.; Kim, S.; Lee, S.; Perez-Neut, M.; et al. Metabolic regulation of gene expression by histone lactylation. *Nature* **2019**, *574*, 575−580.

(14) Hyun, K.; Jeon, J.; Park, K.; Kim, J. Writing, erasing and reading histone lysine methylations. *Exp. Mol. Med.* **2017**, *49*, No. e324.

(15) Bernstein, B. E.; Humphrey, E. L.; Erlich, R. L.; Schneider, R.; Bouman, P.; Liu, J. S.; Kouzarides, T.; Schreiber, S. L. Methylation of histone H3 Lys 4 in coding regions of active genes. *Proc. Natl. Acad. Sci. U.S.A.* **2002**, *99*, 8695−8700.

(16) Klose, R. J.; Yamane, K.; Bae, Y.; Zhang, D.; Erdjument-Bromage, H.; Tempst, P.; Wong, J.; Zhang, Y. The transcriptional repressor JHDM3A demethylates trimethyl histone H3 lysine 9 and lysine 36. *Nature* **2006**, *442*, 312−316.

(17) Greer, E. L.; Shi, Y. Histone methylation: a dynamic mark in health, disease and inheritance. *Nat. Rev. Genet.* **2012**, *13*, 343−357.

(18) Shi, Y.; Lan, F.; Matson, C.; Mulligan, P.; Whetstine, J. R.; Cole, P. A.; Casero, R. A.; Shi, Y. Histone demethylation mediated by the nuclear amine oxidase homolog LSD1. *Cell* **2004**, *119*, 941−953.

(19) Chen, D.; Ma, H.; Hong, H.; Koh, S. S.; Huang, S. M.; Schurter, B. T.; Aswad, D. W.; Stallcup, M. R. Regulation of transcription by a protein methyltransferase. *Science* **1999**, *284*, 2174−2177.

(20) Unnikrishnan, A.; Gafken, P. R.; Tsukiyama, T. Dynamic changes in histone acetylation regulate origins of DNA replication. *Nat. Struct. Mol. Biol.* **2010**, *17*, 430−437.

(21) Kaczmarska, Z.; Ortega, E.; Goudarzi, A.; Huang, H.; Kim, S.; Marquez, J. A.; Zhao, Y.; Khochbin, S.; Panne, D. Structure of p300 in complex with acyl-CoA variants. *Nat. Chem. Biol.* **2017**, *13*, 21−29.

(22) Seto, E.; Yoshida, M. Erasers of histone acetylation: the histone deacetylase enzymes. *Cold Spring Harbor Perspect. Biol.* **2014**, *6*, No. a018713.

(23) Bao, X.; Wang, Y.; Li, X.; Li, X. M.; Liu, Z.; Yang, T.; Wong, C. F.; Zhang, J.; Hao, Q.; Li, X. D. Identification of 'erasers' for lysine crotonylated histone marks using a chemical proteomics approach. *eLife* **2014**, *3*, No. e02999.

(24) Du, J.; Zhou, Y.; Su, X.; Yu, J. J.; Khan, S.; Jiang, H.; Kim, J.; Woo, J.; Kim, J. H.; Choi, B. H.; et al. Sirt5 is a NAD-dependent protein lysine demalonylase and desuccinylase. *Science* **2011**, *334*, 806−809.

(25) Moreno-Yruela, C.; Zhang, D.; Wei, W.; Baek, M.; Liu, W.; Gao, J.; Dankova, D.; Nielsen, A. L.; Bolding, J. E.; Yang, L.; et al. Class I histone deacetylases (HDAC1-3) are histone lysine delactylases. *Sci. Adv.* **2022**, *8*, No. eabi6696.

(26) Ropero, S.; Esteller, M. The role of histone deacetylases (HDACs) in human cancer. *Mol. Oncol.* **2007**, *1*, 19−25.

(27) Falkenberg, K. J.; Johnstone, R. W. Histone deacetylases and their inhibitors in cancer, neurological diseases and immune disorders. *Nat. Rev. Drug Discovery* **2014**, *13*, 673−691.

(28) Namdar, M.; Perez, G.; Ngo, L.; Marks, P. A. Selective inhibition of histone deacetylase 6 (HDAC6) induces DNA damage and sensitizes transformed cells to anticancer agents. *Proc. Natl. Acad. Sci. U.S.A.* **2010**, *107*, 20003−20008.

(29) Whetstine, J. R.; Nottke, A.; Lan, F.; Huarte, M.; Smolikov, S.; Chen, Z.; Spooner, E.; Li, E.; Zhang, G.; Colaiacovo, M.; Shi, Y. Reversal of histone lysine trimethylation by the JMJD2 family of histone demethylases. *Cell* **2006**, *125*, 467−481.

(30) Tsukada, Y.-i.; Fang, J.; Erdjument-Bromage, H.; Warren, M. E.; Borchers, C. H.; Tempst, P.; Zhang, Y. Histone demethylation by a family of JmjC domain-containing proteins. *Nature* **2006**, *439*, 811−816.

(31) Franci, G.; Ciotta, A.; Altucci, L. The Jumonji family: past, present and future of histone demethylases in cancer. *Biomol. Concepts* **2014**, *5*, 209−224.

(32) He, X.; Zhang, H.; Zhang, Y.; Ye, Y.; Wang, S.; Bai, R.; Xie, T.; Ye, X. Y. Drug discovery of histone lysine demethylases (KDMs) inhibitors (progress from 2018 to present). *Eur. J. Med. Chem.* **2022**, *231*, No. 114143.

(33) Jamonnak, N.; Hirsch, B. M.; Pang, Y.; Zheng, W. Substrate specificity of SIRT1-catalyzed lysine Nepsilon-deacetylation reaction probed with the side chain modified Nepsilon-acetyl-lysine analogs. *Bioorg. Chem.* **2010**, *38*, 17−25.

(34) Huang, R.; Holbert, M. A.; Tarrant, M. K.; Curtet, S.; Colquhoun, D. R.; Dancy, B. M.; Dancy, B. C.; Hwang, Y.; Tang, Y.; Meeth, K.; et al. Site-specific introduction of an acetyl-lysine mimic into peptides and proteins by cysteine alkylation. *J. Am. Chem. Soc.* **2010**, *132*, 9986−9987.

(35) Kölle, D.; Brosch, G.; Lechner, T.; Lusser, A.; Loidl, P. Biochemical methods for analysis of histone deacetylases. *Methods* **1998**, *15*, 323−331.

(36) Herman, D.; Jenssen, K.; Burnett, R.; Soragni, E.; Perlman, S. L.; Gottesfeld, J. M. Histone deacetylase inhibitors reverse gene silencing in Friedreich's ataxia. *Nat. Chem. Biol.* **2006**, *2*, 551−558.

(37) Wegener, D.; Wirsching, F.; Riester, D.; Schwienhorst, A. A fluorogenic histone deacetylase assay well suited for high-throughput activity screening. *Chem. Biol.* **2003**, *10*, 61−68.

(38) Rooker, D. R.; Buccella, D. Real-time detection of histone deacetylase activity with a small molecule fluorescent and spectrophotometric probe. *Chem. Sci.* **2015**, *6*, 6456−6461.

(39) Rooker, D. R.; Klyubka, Y.; Gautam, R.; Tomat, E.; Buccella, D. Peptide-Based Fluorescent Probes for Deacetylase and Decrotonylase Activity: Toward a General Platform for Real-Time Detection of Lysine Deacylation. *ChemBioChem* **2018**, *19*, 496−504.

(40) Baba, R.; Hori, Y.; Mizukami, S.; Kikuchi, K. Development of a fluorogenic probe with a transesterification switch for detection of histone deacetylase activity. *J. Am. Chem. Soc.* **2012**, *134*, 14310−14313.

(41) Hori, Y.; Nishiura, M.; Tao, T.; Baba, R.; Bull, S. D.; Kikuchi, K. Fluorogenic probes for detecting deacylase and demethylase activity towards post-translationally-modified lysine residues. *Chem. Sci.* **2021**, *12*, 2498−2503.

(42) Xie, Y.; Chen, L.; Wang, R.; Wang, J.; Li, J.; Xu, W.; Li, Y.; Yao, S. Q.; Zhang, L.; Hao, Q.; Sun, H. Chemical Probes Reveal Sirt2's New Function as a Robust ″Eraser″ of Lysine Lipoylation. *J. Am. Chem. Soc.* **2019**, *141*, 18428−18436.

(43) Xie, Y.; Ge, J.; Lei, H.; Peng, B.; Zhang, H.; Wang, D.; Pan, S.; Chen, G.; Chen, L.; Wang, Y.; et al. Fluorescent Probes for Single-Step Detection and Proteomic Profiling of Histone Deacetylases. *J. Am. Chem. Soc.* **2016**, *138*, 15596−15604.

(44) Xie, Y.; Yang, L.; Chen, Q.; Zhang, J.; Feng, L.; Chen, J. L.; Hao, Q.; Zhang, L.; Sun, H. Single-step fluorescent probes to detect decrotonylation activity of HDACs through intramolecular reactions. *Eur. J. Med. Chem.* **2021**, *212*, No. 113120.

(45) Breinbauer, R.; Kohn, M. Azide-alkyne coupling: a powerful reaction for bioconjugate chemistry. *ChemBioChem* **2003**, *4*, 1147−1149.

(46) Karmodiya, K.; Krebs, A. R.; Oulad-Abdelghani, M.; Kimura, H.; Tora, L. H3K9 and H3K14 acetylation co-occur at many gene regulatory elements, while H3K14ac marks a subset of inactive inducible promoters in mouse embryonic stem cells. *BMC Genomics* **2012**, *13*, No. 424.

(47) Zhou, H.; Finkemeier, I.; Guan, W.; Tossounian, M. A.; Wei, B.; Young, D.; Huang, J.; Messens, J.; Yang, X.; Zhu, J.; et al. Oxidative stress-triggered interactions between the succinyl- and acetyl-proteomes of rice leaves. *Plant Cell Environ.* **2018**, *41*, 1139−1153.

(48) Lain, S.; Hollick, J. J.; Campbell, J.; Staples, O. D.; Higgins, M.; Aoubala, M.; McCarthy, A.; Appleyard, V.; Murray, K. E.; Baker, L.; et al. Discovery, in vivo activity, and mechanism of action of a small-molecule p53 activator. *Cancer Cell* **2008**, *13*, 454−463.

(49) Schuetz, A.; Min, J.; Antoshenko, T.; Wang, C. L.; Allali-Hassani, A.; Dong, A.; Loppnau, P.; Vedadi, M.; Bochkarev, A.; Sternglanz, R.; Plotnikov, A. N. Structural basis of inhibition of the human NAD+-dependent deacetylase SIRT5 by suramin. *Structure* **2007**, *15*, 377−389.

(50) Liu, Y.; Perez, L.; Gill, A. D.; Mettry, M.; Li, L.; Wang, Y.; Hooley, R. J.; Zhong, W. Site-Selective Sensing of Histone Methylation Enzyme Activity via an Arrayed Supramolecular Tandem Assay. *J. Am. Chem. Soc.* **2017**, *139*, 10964−10967.

(51) Forneris, F.; Binda, C.; Vanoni, M. A.; Battaglioli, E.; Mattevi, A. Human histone demethylase LSD1 reads the histone code. *J. Biol. Chem.* **2005**, *280*, 41360−41365.

(52) Forneris, F.; Binda, C.; Dall'Aglio, A.; Fraaije, M. W.; Battaglioli, E.; Mattevi, A. A highly specific mechanism of histone H3-K4 recognition by histone demethylase LSD1. *J. Biol. Chem.* **2006**, *281*, 35289−35295.

(53) Ng, S. S.; Kavanagh, K. L.; McDonough, M. A.; Butler, D.; Pilka, E. S.; Lienard, B. M.; Bray, J. E.; Savitsky, P.; Gileadi, O.; von Delft, F.; et al. Crystal structures of histone demethylase JMJD2A reveal basis for substrate specificity. *Nature* **2007**, *448*, 87−91.

(54) Hillringhaus, L.; Yue, W. W.; Rose, N. R.; Ng, S. S.; Gileadi, C.; Loenarz, C.; Bello, S. H.; Bray, J. E.; Schofield, C. J.; Oppermann, U. Structural and evolutionary basis for the dual substrate selectivity of human KDM4 histone demethylase family. *J. Biol. Chem.* **2011**, *286*, 41616−41625.

(55) Zhang, Y.; Reinberg, D. Transcription regulation by histone methylation: interplay between different covalent modifications of the core histone tails. *Genes Dev.* **2001**, *15*, 2343−2360.

(56) Martin, C.; Zhang, Y. The diverse functions of histone lysine methylation. *Nat. Rev. Mol. Cell Biol.* **2005**, *6*, 838−849.

(57) Hopkinson, R. J.; Hamed, R. B.; Rose, N. R.; Claridge, T. D. W.; Schofield, C. J. Monitoring the activity of 2-oxoglutarate dependent histone demethylases by NMR spectroscopy: direct observation of formaldehyde. *ChemBiochem* **2010**, *11*, 506−510.

(58) Jiang, Y.; Li, Y.; Liu, C.; Zhang, L.; Lv, D.; Weng, Y.; Cheng, Z.; Chen, X.; Zhan, J.; Zhang, H. Isonicotinylation is a histone mark induced by the anti-tuberculosis first-line drug isoniazid. *Nat. Commun.* **2021**, *12*, No. 5548.

📖 **Recommended by ACS**

Molecular Design Strategy of Protein Isoform-Specific Fluorescent Probes by Considering Molecule in Its Entirety

Tienan Zang, Xiaoling Zhang, *et al.*

AUGUST 30, 2023
ANALYTICAL CHEMISTRY   READ ☑

Facile Strategy to Output Fluorescein from Nucleic Acid Interactions

Yeojin Kim, Ki Tae Kim, *et al.*

AUGUST 28, 2023
BIOCONJUGATE CHEMISTRY   READ ☑

Detecting Active Deconjugating Enzymes with Genetically Encoded Activity-Based Ubiquitin and Ubiquitin-like Protein Probes

Xin Shu, Bing Yang, *et al.*

JANUARY 03, 2023
ANALYTICAL CHEMISTRY   READ ☑

Biosensor Optimization Using a Förster Resonance Energy Transfer Pair Based on mScarlet Red Fluorescent Protein and an mScarlet-Derived Green Fluorescent Protein

Khyati Gohil, Robert E. Campbell, *et al.*

JANUARY 24, 2023
ACS SENSORS   READ ☑

Get More Suggestions >